GEOARCHAEOLOGICAL XRF LAB

ARCHAEOLOGICAL X-RAY FLUORESCENCE SPECTROMETRY LABORATORY
8100 WYOMING BLVD., SUITE M4-158 ALBUQUERQUE, NM 87113 USA

# SOURCE PROVENANCE OF OBSIDIAN ARTIFACTS FROM NORTHERN TANZANIA

by

M. Steven Shackley Ph.D., Director
Geoarchaeological XRF Laboratory

Report Prepared for

Dr. Mary Prendergast
Department of Sociology and Anthropology
St. Louis University
Madrid, Spain

26 March 2012

## INTRODUCTION

The analysis here of 36 obsidian artifacts from sites in northern Tanzania is dominated by artifacts produced from a source in Tarangire National Park to the east (55.6%). The remainder of the assemblage exhibits sources from southern Kenya, all of which have very little documentation. Sources of archaeological obsidian in this region are very poorly documented, and there are likely a number of sources that have not yet been reported. Few sources appear in the literature, and much of the data supporting these source assignments was collected many years ago by archaeologists such as Frank Brown and Steven Brandt. More recently Stanley Ambrose has collected samples from a number of sources in the region, but has not yet published the data (J. Ferguson, personal communication).

## LABORATORY SAMPLING, ANALYSIS AND INSTRUMENTATION

All archaeological samples are analyzed whole. The results presented here are quantitative in that they are derived from "filtered" intensity values ratioed to the appropriate x-ray continuum regions through a least squares fitting formula rather than plotting the proportions of the net intensities in a ternary system (McCarthy and Schamber 1981; Schamber 1977). Or more essentially, these data through the analysis of international rock standards, allow for inter-instrument comparison with a predictable degree of certainty (Hampel 1984; Shackley 2011).

All analyses for this study were conducted on a ThermoScientific *Quant'X* EDXRF spectrometer, located in the Archaeological XRF Laboratory, Albuquerque, New Mexico the mirror lab of the NSF sponsored Geoarchaeological XRF Laboratory at the University of California, Berkeley. It is equipped with a thermoelectrically Peltier cooled solid-state Si(Li) X-ray detector, with a 50 kV, 50 W, ultra-high-flux end window bremsstrahlung, Rh target X-ray tube and a 76 μm (3 mil) beryllium (Be) window (air cooled), that runs on a power supply operating 4-50 kV/0.02-1.0 mA at 0.02 increments. The spectrometer is equipped with a 200 l

$min^{-1}$ Edwards vacuum pump, allowing for the analysis of lower-atomic-weight elements between sodium (Na) and titanium (Ti). Data acquisition is accomplished with a pulse processor and an analogue-to-digital converter. Elemental composition is identified with digital filter background removal, least squares empirical peak deconvolution, gross peak intensities and net peak intensities above background.

The analysis for mid Zb condition elements Ti-Nb, Pb, Th, the x-ray tube is operated at 30 kV, using a 0.05 mm (medium) Pd primary beam filter in an air path at 200 seconds livetime to generate x-ray intensity Ka-line data for elements titanium (Ti), manganese (Mn), iron (as $Fe_2O_3^T$), cobalt (Co), nickel (Ni), copper, (Cu), zinc, (Zn), gallium (Ga), rubidium (Rb), strontium (Sr), yttrium (Y), zirconium (Zr), niobium (Nb), lead (Pb), and thorium (Th). Not all these elements are reported since their values in many volcanic rocks are very low. Trace element intensities were converted to concentration estimates by employing a least-squares calibration line ratioed to the Compton scatter established for each element from the analysis of international rock standards certified by the National Institute of Standards and Technology (NIST), the US. Geological Survey (USGS), Canadian Centre for Mineral and Energy Technology, and the Centre de Recherches Pétrographiques et Géochimiques in France (Govindaraju 1994). Line fitting is linear (XML) for all elements but Fe where a derivative fitting is used to improve the fit for iron and thus for all the other elements. When barium (Ba) is analyzed in the High Zb condition, the Rh tube is operated at 50 kV and up to 1.0 mA, ratioed to the bremsstrahlung region (see Davis 2011; Shackley 2011). Further details concerning the petrological choice of these elements in Southwest obsidians is available in Shackley (1988, 1995, 2005; also Mahood and Stimac 1991; and Hughes and Smith 1993). Nineteen specific pressed powder standards are used for the best fit regression calibration for elements Ti-Nb, Pb, Th, and Ba, include G-2 (basalt), AGV-2 (andesite), GSP-2 (granodiorite), SY-2 (syenite), BHVO-2 (hawaiite), STM-1 (syenite), QLO-1 (quartz latite), RGM-1 (obsidian), W-2 (diabase), BIR-1 (basalt), SDC-1 (mica schist), TLM-1 (tonalite), SCO-1 (shale), NOD-A-1 and NOD-P-1 (manganese) all US Geological Survey standards, NIST-278 (obsidian), U.S. National Institute of Standards and Technology, BE-N (basalt) from the Centre de Recherches Pétrographiques et Géochimiques in France, and JR-1 and JR-2 (obsidian) from the Geological Survey of Japan (Govindaraju 1994).

The data from the WinTrace software were translated directly into Excel for Windows software for manipulation and on into SPSS for Windows for statistical analyses. In order to evaluate these quantitative determinations, machine data were compared to measurements of known standards during each run. RGM-1 a USGS obsidian standard is analyzed during each sample run for obsidian artifacts to check machine calibration (Table 1).

## DISCUSSION

A two stage statistical analysis was used to determine source groups, even if some of the source assignments were less certain than I would like. A hierarchical, average linking, Euclidean distance cluster analysis of the artifacts using the elements Zn, Rb, Y, Zr, Nb as variables was imposed on the data producing probable source groups (Figure 1). A scatterplot of Y and Rb was generated both with the dominant Tarangire National Park assigned artifacts and without them, based on the cluster analysis (Figures 2 and 3; Table 2). The scatterplot groups conform to the cluster analysis.

It is important to emphasize, that while the assignments to the Tarangire National Park source appears confident based on data collected by T. Burnette and analyzed by NAA at the University of Missouri Research Reactor, some of the other assignments such as Loirogwa, and Cedar Hill, both in Kenya are less secure. Recent comparison between NAA and XRF has proven favorable (Glascock 2011). This region is in dire need of a source provenance study that is published

## REFERENCES CITED

Davis, K.D., T.L. Jackson, M.S. Shackley, T. Teague, and J.H. Hampel
2011 Factors Affecting the Energy-Dispersive X-Ray Fluorescence (EDXRF) Analysis of Archaeological Obsidian. In *X-Ray Fluorescence Spectrometry (XRF) in Geoarchaeology*, edited by M.S. Shackley, pp. 45-64. Springer, New York.

Glascock, M.D.
2011 Comparison and Contrast Between XRF and NAA: Used for Characterization of Obsidian Sources in Central Mexico. In *X-Ray Fluorescence Spectrometry (XRF) in Geoarchaeology*, edited by M.S. Shackley, pp. 161-182. Springer, New York.

Govindaraju, K.
1994 1994 Compilation of Working Values and Sample Description for 383 Geostandards. *Geostandards Newsletter* 18 (special issue).

Hampel, Joachim H.
1984 Technical Considerations in X-ray Fluorescence Analysis of Obsidian. In *Obsidian Studies in the Great Basin*, edited by R.E. Hughes, pp. 21-25. Contributions of the University of California Archaeological Research Facility 45. Berkeley.

Hildreth, W.
1981 Gradients in Silicic Magma Chambers: Implications for Lithospheric Magmatism. *Journal of Geophysical Research* 86:10153-10192.

Hughes, Richard E., and Robert L. Smith
1993 Archaeology, Geology, and Geochemistry in Obsidian Provenance Studies. *In Scale on Archaeological and Geoscientific Perspectives*, edited by J.K. Stein and A.R. Linse, pp. 79-91. Geological Society of America Special Paper 283.

Mahood, Gail A., and James A. Stimac
1990 Trace-Element Partitioning in Pantellerites and Trachytes. *Geochemica et Cosmochimica Acta* 54:2257- 2276.

McCarthy, J.J., and F.H. Schamber
1981 Least-Squares Fit with Digital Filter: A Status Report. In *Energy Dispersive X-ray Spectrometry*, edited by K.F.J. Heinrich, D.E. Newbury, R.L. Myklebust, and C.E. Fiori, pp. 273-296. National Bureau of Standards Special Publication 604, Washington, D.C.

Schamber, F.H.
1977 A Modification of the Linear Least-Squares Fitting Method which Provides Continuum Suppression. In *X-ray Fluorescence Analysis of Environmental Samples*, edited by T.G. Dzubay, pp. 241-257. Ann Arbor Science Publishers.

Shackley, M. Steven

1988 Sources of Archaeological Obsidian in the Southwest: An Archaeological, Petrological, and Geochemical Study. *American Antiquity* 53(4):752-772.

1990 *Early Hunter-Gatherer Procurement Ranges in the Southwest: Evidence from Obsidian Geochemistry and Lithic Technology*. Ph.D. dissertation, Arizona State University, University Microfilms, Ann Arbor.

1995 Sources of Archaeological Obsidian in the Greater American Southwest: An Update and Quantitative Analysis. *American Antiquity* 60(3):531-551.

2005 *Obsidian: Geology and Archaeology in the North American Southwest*. University of Arizona Press, Tucson.

2011 An Introduction to X-Ray Fluorescence (XRF) Analysis in Archaeology. In *X-Ray Fluorescence Spectrometry (XRF) in Geoarchaeology*, edited by M.S. Shackley, pp. 7-44. Springer, New York.

Table 1. Elemental concentrations and source assignments for the archaeological specimens. All measurements in parts per million (ppm).

| Site/Sample | Ti | Mn | Fe | Zn | Rb | Sr | Y | Zr | Nb | Pb | Th | Source |
|---|---|---|---|---|---|---|---|---|---|---|---|---|
| Jangwanit | | | | | | | | | | | | |
| J2-3-1 | 1172 | 435 | 26562 | 358 | 450 | 12 | 218 | 1584 | 377 | 50 | 80 | Oserian Farm 2, Kenya |
| J2-3-2 | 1466 | 482 | 26643 | 354 | 433 | 12 | 206 | 1536 | 378 | 53 | 75 | Oserian Farm 2, Kenya |
| Mumba | | | | | | | | | | | | |
| MUMBA-1 | 1480 | 486 | 26989 | 410 | 438 | 22 | 202 | 1497 | 365 | 51 | 69 | Oserian Farm 2, Kenya |
| MUMBA-2 | 1169 | 330 | 15707 | 201 | 303 | 17 | 101 | 450 | 200 | 27 | 43 | Tarangire Natl Park, Tanzania |
| MUMBA-3 | 1139 | 439 | 25993 | 351 | 446 | 12 | 204 | 1548 | 380 | 48 | 74 | Oserian Farm 1, Kenya |
| MUMBA-4 | 1092 | 349 | 15892 | 188 | 317 | 16 | 105 | 453 | 205 | 27 | 45 | Tarangire Natl Park, Tanzania |
| MUMBA-5 | 1130 | 310 | 14835 | 199 | 299 | 19 | 100 | 441 | 195 | 24 | 41 | Tarangire Natl Park, Tanzania |
| Sonai | | | | | | | | | | | | |
| SONAI-1 | 1090 | 308 | 14150 | 212 | 274 | 15 | 87 | 416 | 185 | 23 | 38 | Tarangire Natl Park, Tanzania |
| SONAI-2 | 2077 | 1681 | 59259 | 574 | 229 | 21 | 227 | 1530 | 342 | 31 | 30 | Masai Gorge, Kenya? |
| SONAI-3 | 1882 | 1659 | 53977 | 534 | 219 | 17 | 171 | 1049 | 253 | 26 | 36 | Eburru, Kenya |
| SONAI-4 | 1133 | 348 | 15603 | 266 | 304 | 26 | 95 | 436 | 197 | 28 | 51 | Tarangire Natl Park, Tanzania |
| SONAI-5 | 1093 | 339 | 15870 | 156 | 319 | 14 | 107 | 467 | 207 | 28 | 48 | Tarangire Natl Park, Tanzania |
| Daumboy | | | | | | | | | | | | |
| DAUMBOY-1 | 1315 | 498 | 28802 | 389 | 466 | 13 | 211 | 1583 | 387 | 51 | 77 | Oserian Farm 1, Kenya |
| Semonyati | | | | | | | | | | | | |
| SEMONYATI-1 | 1916 | 1739 | 58205 | 511 | 226 | 17 | 245 | 1585 | 363 | 31 | 37 | Masai Gorge, Kenya? |
| Gileodabeshta | | | | | | | | | | | | |
| G2-1-1 | 1121 | 290 | 13674 | 140 | 282 | 14 | 99 | 444 | 207 | 21 | 42 | Tarangire Natl Park, Tanzania |
| G2-1-2 | 1025 | 295 | 13745 | 115 | 294 | 11 | 102 | 443 | 196 | 24 | 41 | Tarangire Natl Park, Tanzania |
| G2-1-3 | 1435 | 1230 | 43609 | 350 | 208 | 18 | 177 | 1112 | 268 | 20 | 29 | Loirogwa, Kenya? |
| G2-1-4 | 1113 | 317 | 15146 | 147 | 301 | 14 | 99 | 451 | 205 | 25 | 47 | Tarangire Natl Park, Tanzania |
| G2-1-5 | 1094 | 342 | 16127 | 153 | 322 | 13 | 108 | 480 | 212 | 30 | 49 | Tarangire Natl Park, Tanzania |
| G2-4-1 | 1153 | 329 | 15846 | 188 | 311 | 12 | 104 | 465 | 206 | 21 | 41 | Tarangire Natl Park, Tanzania |
| G2-4B-1 | 1105 | 345 | 15390 | 154 | 302 | 13 | 100 | 458 | 206 | 24 | 47 | Tarangire Natl Park, Tanzania |
| G2-4B-2 | 1123 | 341 | 16200 | 165 | 307 | 13 | 101 | 455 | 205 | 28 | 44 | Tarangire Natl Park, Tanzania |
| G2-4B-3 | 100 | 290 | 1438 | 13 | 29 | 14 | 98 | 442 | 20 | 24 | 41 | Tarangire Natl Park, |

| | | | | | | | | | | | | |
|---|---|---|---|---|---|---|---|---|---|---|---|---|
| | 0 | | 0 | 5 | 8 | | | | 5 | | | Tanzania |
| G2-4B-4 | 1069 | 314 | 15033 | 157 | 301 | 15 | 102 | 451 | 211 | 25 | 46 | Tarangire Natl Park, Tanzania |
| G2-4B-5 | 1061 | 319 | 15682 | 160 | 311 | 15 | 99 | 465 | 211 | 28 | 45 | Tarangire Natl Park, Tanzania |
| G2-4B-6 | 2047 | 1898 | 63869 | 518 | 261 | 19 | 202 | 1245 | 300 | 29 | 37 | Cedar Hill, Kenya? |
| G2-4B-7 | 1877 | 1804 | 58433 | 489 | 237 | 18 | 255 | 1649 | 379 | 29 | 33 | Masai Gorge, Kenya |
| G2-4B-8 | 1088 | 327 | 15494 | 139 | 304 | 15 | 103 | 457 | 204 | 25 | 47 | Tarangire Natl Park, Tanzania |
| G2-4-2 | 2236 | 1872 | 62152 | 551 | 223 | 21 | 237 | 1536 | 350 | 31 | 31 | Masai Gorge, Kenya |
| G2-4-3 | 2172 | 1955 | 65559 | 540 | 243 | 20 | 252 | 1654 | 377 | 34 | 42 | Masai Gorge, Kenya |
| G2-4-4 | 2044 | 1859 | 61208 | 521 | 235 | 21 | 246 | 1612 | 373 | 26 | 32 | Masai Gorge, Kenya |
| G2-4-5 | 1179 | 333 | 15716 | 163 | 318 | 13 | 101 | 465 | 210 | 24 | 51 | Tarangire Natl Park, Tanzania |
| G2-4.6 | 1789 | 1931 | 63295 | 513 | 263 | 19 | 202 | 1258 | 299 | 25 | 41 | Cedar Hill, Kenya? |
| G2-4-7 | 1239 | 309 | 15195 | 193 | 288 | 18 | 99 | 439 | 199 | 23 | 40 | Tarangire Natl Park, Tanzania |
| G2-4-8 | 1083 | 334 | 14967 | 168 | 301 | 13 | 100 | 439 | 202 | 22 | 41 | Tarangire Natl Park, Tanzania |
| RGM1-S4 | 1662 | 303 | 13253 | 35 | 151 | 106 | 24 | 221 | 7 | 21 | 16 | standard |
| RGM1-S4 | 1631 | 284 | 13243 | 35 | 150 | 112 | 22 | 215 | 10 | 21 | 19 | standard |

Table 2. Crosstabulation of site by source.

| | | | Site | | | | | | |
|---|---|---|---|---|---|---|---|---|---|
| | | | Daumboy | Gileodabeshta | Jangwanit | Mumba | Semonyati | Sonai | Total |
| Source | | Count | 0 | 1 | 0 | 0 | 0 | 0 | 1 |
| | | % within Source | .0% | 100.0% | .0% | .0% | .0% | .0% | 100.0% |
| | | % within Site/Sample | .0% | 4.5% | .0% | .0% | .0% | .0% | 2.8% |
| | | % of Total | .0% | 2.8% | .0% | .0% | .0% | .0% | 2.8% |
| | Cedar Hill, Kenya? | Count | 0 | 2 | 0 | 0 | 0 | 0 | 2 |
| | | % within Source | .0% | 100.0% | .0% | .0% | .0% | .0% | 100.0% |
| | | % within Site/Sample | .0% | 9.1% | .0% | .0% | .0% | .0% | 5.6% |
| | | % of Total | .0% | 5.6% | .0% | .0% | .0% | .0% | 5.6% |
| | Eburru, Kenya | Count | 0 | 0 | 0 | 0 | 0 | 1 | 1 |
| | | % within Source | .0% | .0% | .0% | .0% | .0% | 100.0% | 100.0% |
| | | % within Site/Sample | .0% | .0% | .0% | .0% | .0% | 20.0% | 2.8% |
| | | % of Total | .0% | .0% | .0% | .0% | .0% | 2.8% | 2.8% |
| | Loirogwa, Kenya? | Count | 0 | 1 | 0 | 0 | 0 | 0 | 1 |
| | | % within Source | .0% | 100.0% | .0% | .0% | .0% | .0% | 100.0% |
| | | % within Site/Sample | .0% | 4.5% | .0% | .0% | .0% | .0% | 2.8% |
| | | % of Total | .0% | 2.8% | .0% | .0% | .0% | .0% | 2.8% |
| | Masai Gorge, Kenya | Count | 0 | 4 | 0 | 0 | 0 | 0 | 4 |
| | | % within Source | .0% | 100.0% | .0% | .0% | .0% | .0% | 100.0% |
| | | % within Site/Sample | .0% | 18.2% | .0% | .0% | .0% | .0% | 11.1% |
| | | % of Total | .0% | 11.1% | .0% | .0% | .0% | .0% | 11.1% |
| | Masai Gorge, Kenya? | Count | 0 | 0 | 0 | 0 | 1 | 1 | 2 |
| | | % within Source | .0% | .0% | .0% | .0% | 50.0% | 50.0% | 100.0% |
| | | % within Site/Sample | .0% | .0% | .0% | .0% | 100.0% | 20.0% | 5.6% |
| | | % of Total | .0% | .0% | .0% | .0% | 2.8% | 2.8% | 5.6% |
| | Oserian Farm 1, Kenya | Count | 1 | 0 | 0 | 1 | 0 | 0 | 2 |
| | | % within Source | 50.0% | .0% | .0% | 50.0% | .0% | .0% | 100.0% |
| | | % within Site/Sample | 100.0% | .0% | .0% | 20.0% | .0% | .0% | 5.6% |
| | | % of Total | 2.8% | .0% | .0% | 2.8% | .0% | .0% | 5.6% |
| | Oserian Farm 2, Kenya | Count | 0 | 0 | 2 | 1 | 0 | 0 | 3 |
| | | % within Source | .0% | .0% | 66.7% | 33.3% | .0% | .0% | 100.0% |
| | | % within Site/Sample | .0% | .0% | 100.0% | 20.0% | .0% | .0% | 8.3% |
| | | % of Total | .0% | .0% | 5.6% | 2.8% | .0% | .0% | 8.3% |
| | Tarangire Natl Park, Tanzania | Count | 0 | 14 | 0 | 3 | 0 | 3 | 20 |
| | | % within Source | .0% | 70.0% | .0% | 15.0% | .0% | 15.0% | 100.0% |
| | | % within Site/Sample | .0% | 63.6% | .0% | 60.0% | .0% | 60.0% | 55.6% |
| | | % of Total | .0% | 38.9% | .0% | 8.3% | .0% | 8.3% | 55.6% |
| Total | | Count | 1 | 22 | 2 | 5 | 1 | 5 | 36 |
| | | % within Source | 2.8% | 61.1% | 5.6% | 13.9% | 2.8% | 13.9% | 100.0% |
| | | % within Site/Sample | 100.0% | 100.0% | 100.0% | 100.0% | 100.0% | 100.0% | 100.0% |
| | | % of Total | 2.8% | 61.1% | 5.6% | 13.9% | 2.8% | 13.9% | 100.0% |

Figure 1. Hierarchical, average linking, Euclidean distance cluster analysis of the artifacts using the elements Zn, Rb, Y, Zr, Nb as variables.

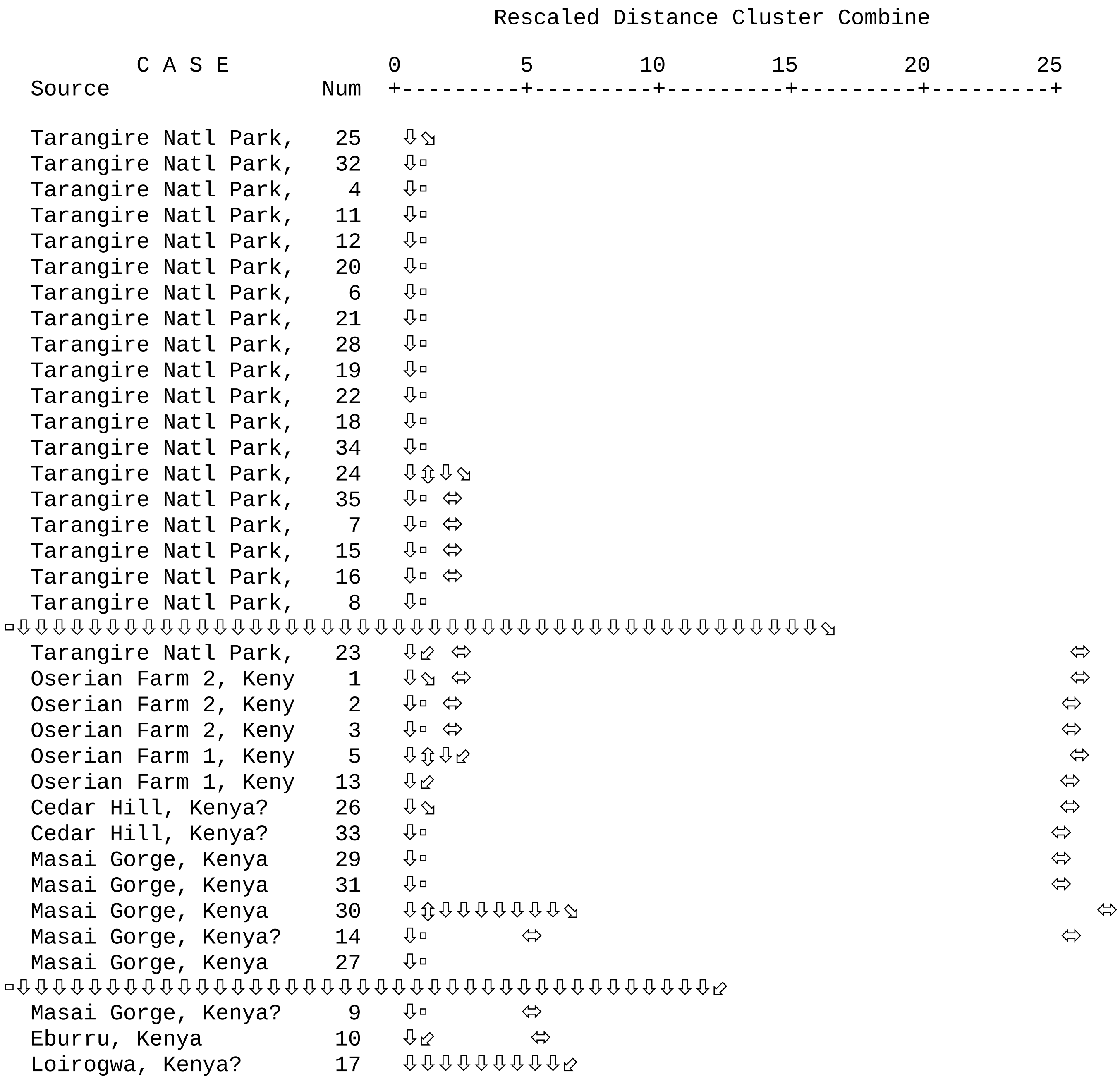

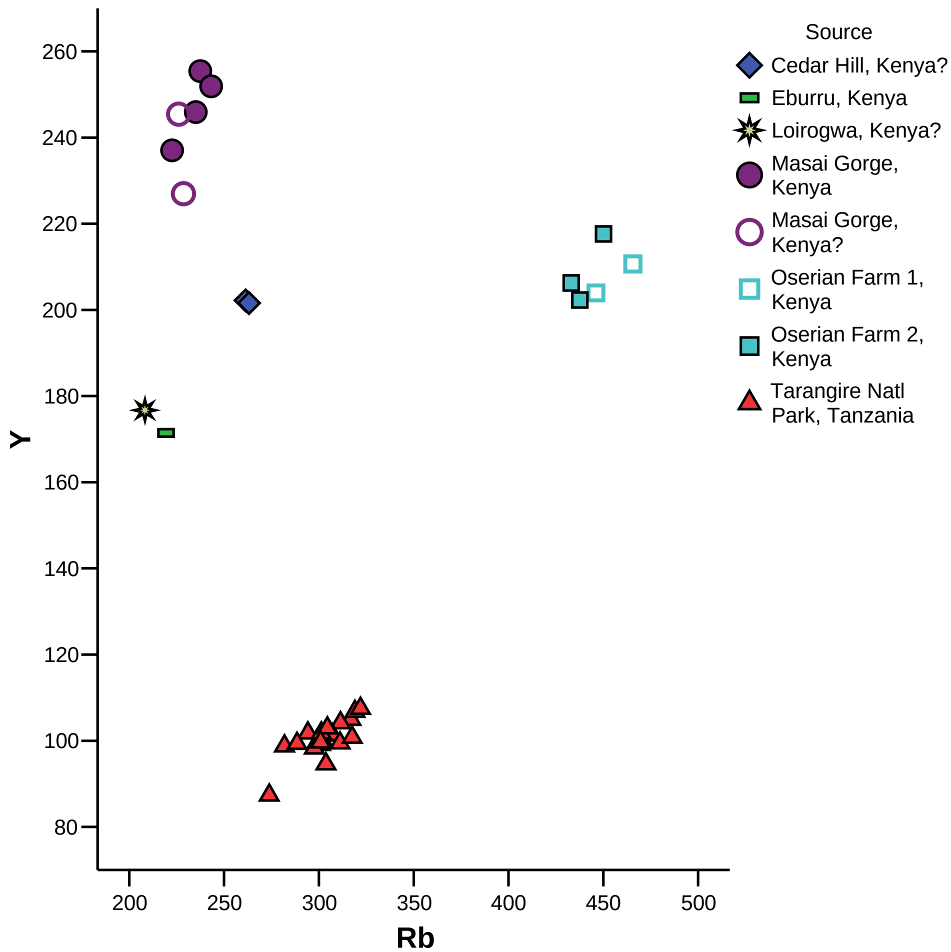


Figure 2. Rb versus Y bivariate plot of the elemental concentrations for all the archaeological specimens.

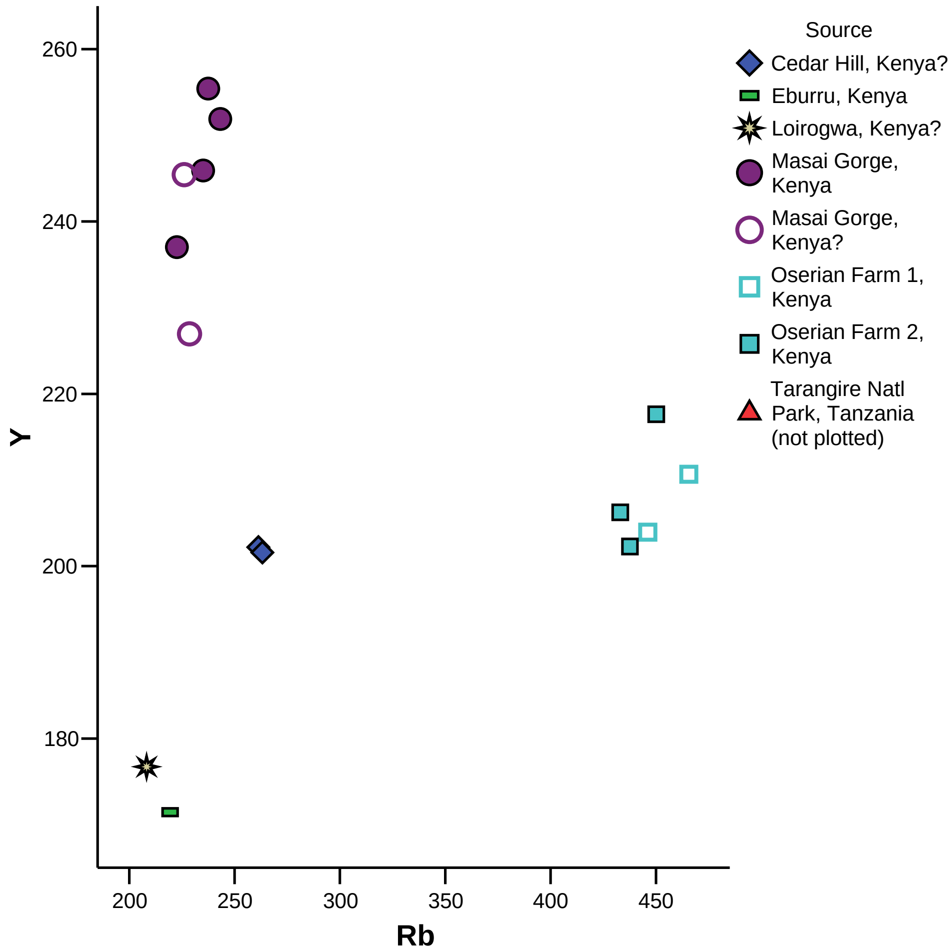


Figure 2. Rb versus Y bivariate plot of the elemental concentrations for the archaeological specimens with the Tarangire National Park specimens deleted to provide clarity.